

Optical vortex solitons in parametric wave mixing

Tristram J. Alexander,¹ Yuri S. Kivshar,¹ Alexander V. Buryak,^{1,2} and Rowland A. Sammut²

¹*Optical Sciences Center, Research School of Physical Sciences and Engineering, Australian National University, Canberra ACT 0200, Australia*

²*School of Mathematics and Statistics, Australian Defence Force Academy, Canberra ACT 2600, Australia*

(Received 8 March 1999)

We analyze *two-component spatial optical vortex solitons* supported by parametric wave mixing processes in a nonlinear bulk medium. We study two distinct cases of such localized waves, namely, parametric vortex solitons due to phase-matched second-harmonic generation in an optical medium with competing *quadratic* and *cubic* nonlinear response, and vortex solitons in the presence of *third-harmonic generation* in a cubic medium. We find, analytically and numerically, the structure of two-component vortex solitons, and also investigate modulational instability of their plane-wave background. In particular, we predict and analyze in detail *novel types* of vortex solitons, a “*halo-vortex*,” consisting of a two-component vortex core surrounded by a bright ring of its harmonic field, and a “*ring-vortex*” soliton which is a vortex in a harmonic field that guides a ring-like localized mode of the fundamental-frequency field.

PACS number(s): 42.65.Tg, 42.65.Jx, 42.65.Ky, 41.20.Jb

I. INTRODUCTION

An optical vortex soliton appears as a stationary self-trapped beam in a self-defocusing optical medium that carries a phase singularity on an electromagnetic field, so that the beam intensity vanishes at a certain point, and the field phase changes by $2\pi m$ (m being integer) along any closed loop around the zero-intensity point. If such an object is created in a linear bulk medium [1,2], it preserves the singularity but expands due to diffraction. However, in a nonlinear medium, the diffraction-induced expansion of the vortex core can be compensated for by a nonlinearity-induced change in the refractive index of a nonlinear medium, thereby creating a stationary self-trapped structure, an *optical vortex soliton*. Such nonlinear localized waves carrying a singularity were first introduced as stationary solutions of the nonlinear Schrödinger (NLS) equation in the pioneering paper by Ginzburg and Pitaevsky [3] to describe topological excitations in superfluids, but the same objects appear in many other fields [4] including nonlinear optics [5].

The parametric interactions may provide an efficient way of vortex transformation. In particular, by mixing waves of different frequencies, one can change the vortex topological charge m and even the vortex polarization. Recently, the first experimental results on the vortex generation in the presence of two-wave parametric mixing have been reported in nonlinear optics, including the second-harmonic generation (SHG) [6,7] and more general types of frequency conversion [8] and sum-frequency mixing [9] where the generation of higher-order ($|m| > 1$) linear vortices in the case of negligible spatial walk-off between harmonics was demonstrated.

To the best of our knowledge, no theory of parametric optical vortices in the presence of both diffraction and nonlinearity has been developed so far. In a nonlinear regime, an interplay between diffraction and parametric coupling of the harmonic fields is expected to lead to the formation of stationary structures — *parametric vortex solitons* — supported by three- or four-wave mixing between the phase-matched waves of different frequencies. Stability of such multifre-

quency vortex solitons is a key issue. For example, in the problem of SHG in a diffractive bulk medium, vortex solitons are expected to be unstable due to parametric modulational instability of the two-wave background field [10]. Recently, it has been suggested [11] that taking into account a *weak defocusing cubic nonlinearity* one can eliminate the development of parametric modulational instability allowing stable dark solitons to exist. Some examples of stable two-wave parametric dark solitons have been presented in Ref. [11], and it has been pointed out that, in the problem of SHG, a stable vortex soliton of the lowest possible charge ($|m|=1$) can exist describing a 2π -phase twist of the fundamental wave and 4π -phase twist in the second-harmonic field.

In the present paper, we suggest a general approach to the analysis of *multicomponent vortex solitons* resulting from parametric wave mixing. The general theory is then developed in detail in the no-walkoff case for *two examples*: (i) parametric interaction of the first and second harmonics in a medium with competing quadratic and cubic nonlinearity, and (ii) parametric interaction between the first and third harmonics in a medium with a cubic nonlinear response. In both the cases, we find different classes of vortex solitons as $(2+1)$ -dimensional dark solitons of circular symmetry carrying a phase singularity, and investigate their stability to propagation and modulational stability of the supporting two-component background waves.

The paper is organized as follows. In Sec. II, we briefly present two models of parametric wave interaction that describe a phase-matched coupling between the fundamental frequency mode and its harmonic field, in the case of phase-matched wave mixing and no walk-off. The further analysis of the asymptotic structure of stationary localized solutions for parametric vortex solitons is rather general, and it is presented in Sec. III for both the models. Section IV is devoted to the analysis of vortex solitons in the model of competing nonlinearities. We find numerically the profiles of two-component vortex solitons and investigate their stability to propagation. In particular, we reveal the existence of classes

of dark-soliton solutions of radial symmetry, including a *ring-vortex soliton*, that consists of a vortex core in the harmonic field surrounded by a bright ring of its fundamental frequency, and a *halo-vortex*, a two-wave vortex soliton with nonmonotonic tails. The corresponding results are also obtained for the problem of the third-harmonic generation in Sec. V. Finally, Sec. VI gives the summary of our results and briefly discusses some related issues including the comments on experimental verifications and a link with other problems.

II. MODELS OF TWO-WAVE PARAMETRIC INTERACTION

A. Competing nonlinearities

First, we consider the model of competing quadratic and cubic nonlinearities introduced earlier for the (1+1)-dimensional case in Ref. [12] and recently generalized to the case of (2+1)-dimensional bright solitons of radial symmetry in a bulk medium [13]. We assume that a beam of a fundamental harmonic (FH) with the frequency ω is launched into a medium possessing combined quadratic (or $\chi^{(2)}$) and cubic (or $\chi^{(3)}$) nonlinear response under the condition of phase-matched SHG. The FH beam generates a second harmonic (SH) wave, and such a two-wave mixing process in a bulk medium is described by a system of two coupled nonlinear equations,

$$\begin{aligned} 2ik_1 \frac{\partial E_1}{\partial z} + \nabla_{\perp}^2 E_1 + \frac{8\pi\omega^2}{c^2} \chi^{(2)} E_2 E_1^* e^{-i\Delta kz} \\ + \frac{12\pi\omega^2}{c^2} \chi^{(3)} (|E_1|^2 + \rho |E_2|^2) E_1 = 0, \\ 4ik_1 \frac{\partial E_2}{\partial z} + \nabla_{\perp}^2 E_2 + \frac{16\pi\omega^2}{c^2} \chi^{(2)} E_1^2 e^{i\Delta kz} \\ + \frac{48\pi\omega^2}{c^2} \chi^{(3)} (|E_2|^2 + \rho |E_1|^2) E_2 = 0, \end{aligned} \quad (1)$$

where E_1 and E_2 are the complex amplitude envelopes of FH ($\omega_1 = \omega$) and SH ($\omega_2 = 2\omega$) waves, respectively; $k_1 = k(\omega)$ and $k_2 = k(2\omega)$ are the corresponding wave numbers; $\Delta k \equiv (2k_1 - k_2)$ is the wave-vector mismatch between the harmonics, ρ (which we take $\rho = 2$) is the cross-phase-modulation coefficient, and the coefficients $\chi^{(2)}$ and $\chi^{(3)}$ are proportional to the second- and third-order susceptibility tensor elements and they characterize the combined nonlinear response of an optical medium.

Adopting a similar set of scaling transformations as in Ref. [13], we measure the transverse coordinates in the units of the beam radius R_0 , and the propagation coordinate, in the units of the beam diffraction length $R_d = 2k_1 R_0^2$. Then, applying the transformations

$$\begin{aligned} E_1 &= \beta c^2 (16\pi\omega^2 \chi^{(2)} R_0^2)^{-1} e^{i\beta z} u(x, y, z), \\ E_2 &= \beta c^2 (8\pi\omega^2 \chi^{(2)} R_0^2)^{-1} e^{i[(2\beta + \Delta)z]} w(x, y, z), \end{aligned}$$

where the parameter β stands for the nonlinearity-induced change of the beam propagation constant and $\Delta = 2k_1 R_d^2 \Delta k$, we obtain a system of normalized equations for u and w ,

$$\begin{aligned} i \frac{\partial u}{\partial z} + s \nabla_{\perp}^2 u - u + w u^* + \chi \left(\frac{|u|^2}{2\sigma} + \rho |w|^2 \right) u = 0, \\ i \sigma \frac{\partial w}{\partial z} + s \nabla_{\perp}^2 w - \alpha w + \frac{u^2}{2} + \chi (2\sigma |w|^2 + \rho |u|^2) w = 0, \end{aligned} \quad (2)$$

where $\alpha = (2\beta + \Delta)\sigma/\beta$, $s \equiv \text{sign } \beta$, and the coordinates are rescaled as follows $z \rightarrow z/\beta$ and $(x, y) \rightarrow (x, y)/\sqrt{|\beta|}$. For the spatial beam propagation we take $\sigma = 2$. Parameter χ describes a competition between quadratic and cubic nonlinearities, and it is defined as

$$\chi = \beta \frac{3c^2}{16\pi\omega_1^2 R_0^2} \frac{\chi^{(3)}}{[\chi^{(2)}]^2}. \quad (3)$$

Stationary solutions are then described by Eq. (2) with the z -derivatives omitted. To look for radially symmetric solutions carrying a phase singularity, we use the polar coordinates $r = \sqrt{x^2 + y^2}$, $\phi = \tan^{-1}(x/y)$, and make the following substitutions,

$$u(r, \phi) = U(r) e^{im\phi}, \quad w(r, \phi) = W(r) e^{iNm\phi}, \quad (4)$$

where $U(r)$ and $W(r)$ are real functions and, for parametric interaction between the fundamental and second harmonics, $N = 2$ whereas m is an integer number that characterizes the vortex charge.

Substituting Eq. (4) into Eq. (2), we obtain

$$\begin{aligned} \frac{d^2 U}{dr^2} + \frac{1}{r} \frac{dU}{dr} - \frac{m^2 U^2}{r^2} + s \frac{\partial F}{\partial U} = 0, \\ \frac{d^2 W}{dr^2} + \frac{1}{r} \frac{dW}{dr} - \frac{m^2 N^2 W^2}{r^2} + s \frac{\partial F}{\partial W} = 0, \end{aligned} \quad (5)$$

where the function F has the meaning of an effective potential, and it is defined as

$$\begin{aligned} F = F_1(U, W) = -\frac{1}{2} U^2 + \frac{1}{2} U^2 W - \frac{\alpha}{2} W^2 \\ + \chi \left(\frac{1}{16} U^4 + W^4 + \frac{1}{2} \rho W^2 U^2 \right). \end{aligned} \quad (6)$$

B. Third-harmonic generation

A similar type of two-wave parametric interaction occurs under the condition of the third-harmonic generation. Bright and dark solitary waves in a waveguide geometry (i.e., with one transverse dimension) have been analyzed in Ref. [14]. In this case, the parametric interaction occurs between the fundamental beam ($\omega_1 = \omega$) and its third harmonic ($\omega_3 = 3\omega$), and the corresponding physical model of the parametric wave mixing in a bulk can be described by a system of two coupled equations,

$$\begin{aligned}
& 2ik_1 \frac{\partial E_1}{\partial z} + s \nabla^2 E_1 - \chi [(|E_1|^2 + 2|E_3|^2) E_1 + E_1^{*2} E_3 e^{-i\Delta kz}] \\
& = 0, \\
& 2ik_3 \frac{\partial E_3}{\partial z} + s \nabla^2 E_3 - 9\chi \left[(|E_3|^2 + 2|E_1|^2) E_3 + \frac{1}{3} E_1^3 E_3 e^{i\Delta kz} \right] \\
& = 0,
\end{aligned} \tag{7}$$

where E_1 and E_3 are the slowly varying envelopes of the first and third harmonic fields, respectively, with corresponding wave numbers $k_1 = k(\omega)$ and $k_3 = k(3\omega)$; $\Delta k = 3k_1 - k_3$ is the wave-vector mismatch between the harmonics and $\chi = (3\pi\omega^2/c^2)|\chi^{(3)}|$ is the nonlinearity parameter, which is assumed here to be always positive, whereas $\chi^{(3)} < 0$.

We follow a normalization procedure similar to that used above for the competing nonlinearity model. Again, the transverse coordinate is measured in units of the beam width R_0 and the propagation coordinate, in units of the diffraction length $R_d = 2k_1 R_0^2$. Using the transformations of Ref. [14]

$$\begin{aligned}
E_1 &= (\sqrt{\beta/3} \sqrt{k_1 R_0^2 \chi}) e^{i\beta z} u(x, y, z), \\
E_2 &= (\sqrt{\beta}/\sqrt{k_1 R_0^2 \chi}) e^{i(3\beta + \Delta)z} w(x, y, z),
\end{aligned} \tag{8}$$

the physical Eq. (7) can be written in the following normalized form [cf. Eq. (2)],

$$\begin{aligned}
i \frac{\partial u}{\partial z} + s \nabla^2 u - u - \frac{s}{3} u^{*2} w - s \left(\frac{|u|^2}{9} + 2|w|^2 \right) u &= 0, \\
i \sigma \frac{\partial w}{\partial z} + s \nabla^2 w - \alpha w - \frac{s}{9} u^3 - s(9|w|^2 + 2|u|^2) w &= 0,
\end{aligned} \tag{9}$$

where u and w are the normalized amplitudes of the fundamental harmonic field and its third harmonic, $\alpha = \sigma(3\beta + \Delta)/\beta$, $\Delta = 2k_1 R_0^2 \Delta k$, $s \equiv \text{sgn } \beta$, the transverse and propagation coordinates have been rescaled in terms of the nonlinearity-induced change of the propagation constant β , $z \rightarrow z/\beta$ and $(x, y) \rightarrow (x, y)/\sqrt{|\beta|}$, and, for spatial solitons, we take $\sigma = 3$. Importantly, everywhere below we consider only *defocusing cubic nonlinearity* searching for vortex-type solitary waves on a modulationally stable nonvanishing background.

Stationary radially symmetric localized solutions of Eq. (9) have the form (4) with $N = 3$, and they satisfy Eq. (5) with the potential F , this time defined as

$$\begin{aligned}
F = F_2(U, W) &= -\frac{1}{2} U^2 - \frac{\alpha}{2} W^2 - s \\
&\times \left(\frac{1}{9} U^3 W + \frac{1}{36} U^4 + \frac{9}{4} W^4 + W^2 U^2 \right).
\end{aligned} \tag{10}$$

Thus, in both the cases, stationary vortex-like structures are described by the same system of Eq. (5) with different types of the potential F . This observation allows us to perform further analytical calculations in a rather general form, and, therefore, most of them are universal and can be applied to other models.

III. GENERAL THEORY OF PARAMETRIC VORTEX SOLITONS

A. Stationary solutions

Stationary radially symmetric solutions of Eq. (2) [Eq. (9)] are given by Eq. (5) with the potential function F defined in Eq. (6) [Eq. (10)] and $N = 2$ [$N = 3$]. It is important to note that the parametric coupling between the modes brings *several features* in the vortex structure and properties. Indeed, as follows from Eqs. (4) and (5), a vortex with the charge m in the fundamental mode is always coupled to a vortex of the charge Nm ($N = 2, 3$) in the harmonic component. This makes parametric vortices very different from all types of vortex solitons analyzed earlier in the systems of two incoherently coupled NLS equations (see, e.g., Ref. [15] and references therein).

B. Analysis of vortex asymptotics

We are interested in the localized solutions supported by a two-component finite-amplitude background wave. For $r \rightarrow \infty$, the background amplitudes (U_0, W_0) satisfy the coupled algebraic equations:

$$\frac{\partial F}{\partial U} = 0, \quad \frac{\partial F}{\partial W} = 0, \tag{11}$$

which may have one or more nontrivial solutions. Importantly, due to the self-action effect we always have a special solution of the form $(0, W_0)$, that corresponds to an excited harmonic field only.

A vortex soliton is a localized nonlinear mode that asymptotically approaches the background (U_0, W_0) for $r \rightarrow \infty$, but its intensity vanishes for $r \rightarrow 0$ to keep the terms $\sim (m^2/r^2)U$ and $\sim (m^2 N^2/r^2)W$ in Eq. (5) finite. This implies that we can find the vortex asymptotics in a rather general form. For $r \rightarrow 0$, we look for solutions of Eq. (5) in the form:

$$U = U_0 - \frac{A}{r^2} - \frac{A_2}{r^4} + \dots, \tag{12}$$

$$W = W_0 - \frac{B}{r^2} - \frac{B_2}{r^4} + \dots,$$

where (U_0, W_0) is a solution of Eq. (11) for the background amplitudes. Keeping in Eq. (5) only the asymptotic terms up to the order of $\sim 1/r^2$, we obtain,

$$sm^2 U_0 + \left(\frac{\partial^2 F}{\partial U^2} \right)_0 A + \left(\frac{\partial^2 F}{\partial U \partial W} \right)_0 B = 0, \tag{13}$$

$$sN^2 m^2 W_0 + \left(\frac{\partial^2 F}{\partial W^2} \right)_0 B + \left(\frac{\partial^2 F}{\partial W \partial U} \right)_0 A = 0,$$

where the index 0 stands for the values calculated at $U = U_0$ and $W = W_0$. Solutions of the linear Eq. (13) for A and B can be easily found analytically; they define the asymptot-

ics of the vortex solitons for different values of the vortex charge m in terms of the background amplitudes U_0 and W_0 defined by Eqs. (11).

The analysis of the asymptotics gives us important information about the vortex structure. If both the products AU_0 and BW_0 are positive [see Eq. (12)], the vortex has a standard profile with the intensity in the core growing monotonically and always lower than the background intensity. However, if one of these products is negative, somewhere across the vortex the intensity becomes higher than the asymptotic background intensity. That implies that the vortex core is surrounded by a bright ring of higher intensity. We call such structures “*halo-vortices*.” In both the cases mentioned above, such vortex solitons may exist on a modulationally stable background, and some examples are given below in Secs. IV and V.

C. Vortex soliton as a waveguide

The concept of light guiding light (see e.g., Ref. [16] and references therein) is based on a simple observation that a spatial optical soliton (e.g., vortex) creates an effective optical waveguide in a nonlinear medium that can guide a wave of different frequency or polarization. It is clear that a vortex soliton creates a waveguide of radial symmetry, which can guide a fundamental mode (no nodes) of the other wave. For the case of two incoherently coupled NLS equations describing two orthogonal polarizations, the guiding properties of vortex solitons have been analyzed by Haelterman and Shepard [15]. The first demonstration of an optically written waveguide based on an optical vortex has been recently reported by Truscott *et al.* [17]. However, the theory developed in Ref. [15] is not valid for the case of the resonant interactions and parametrically coupled waves. Indeed, the parametric interaction forces the harmonic field to vanish for $r \rightarrow 0$, *trapping a singularity* of the order of Nm . Therefore, a parametric vortex *cannot guide a fundamental mode*. To analyze the guiding properties of parametric vortex solitons, we note that Eqs. (11) with the potential F defined by Eqs. (6) and (10) have the solution ($U_0=0, W_0 \neq 0$). Therefore, we consider a vortex soliton created by a harmonic field W , with a stationary profile described by the nonlinear equation,

$$\frac{d^2W}{dr^2} + \frac{1}{r} \frac{dW}{dr} - \left(\frac{N^2m^2}{r^2} + s\alpha \right) W - \gamma W^3 = 0,$$

where $\gamma = -4s\chi$, for the model (2), and $\gamma = 9$, for the model (9). This equation always has a solution in the form of a vortex soliton with the charge Nm provided $\gamma > 0$ and $s\alpha < 0$. Now, an eigenvalue equation for a linear mode guided by the vortex $W(r)$ follows from the first equation of the system (5). Assuming $U \ll \max(W)$, we obtain,

$$\frac{d^2U}{dr^2} + \frac{1}{r} \frac{dU}{dr} - \left[\frac{m^2}{r^2} + s - sG(r) \right] U = 0, \quad (14)$$

where

$$G(r) = \left(\frac{d^2F}{dU^2} \right) \Big|_{U=0}.$$

Equation (14) is a standard eigenvalue problem of the linear waveguide theory, and it can be studied analytically, e.g., by means of variational methods (see, e.g., Ref. [18] and references therein). To make some analytical estimates, we present $G(r)$ in an approximate form and obtain

$$\frac{d^2U}{dr^2} + \frac{1}{r} \frac{dU}{dr} - \frac{m^2}{r^2} U - EU + \frac{C^2}{(D^2 + r^2)} U = 0,$$

where E, C , and D are, in general, functions of α and γ . The parameters are chosen to provide the best approximation of the effective potential $G(r)$. Using the standard variational method (or Ritz optimization approach) and looking for a bifurcation of a linear mode taken in a trial form, $f(r) = r \exp(-\kappa r)$, we obtain an implicit expression to determine the mode cutoff α ,

$$E = (2C^2 - 1 - 2m^2)^3 / (36C^4D^2),$$

which we analyze below for some particular cases.

D. Modulational instability

Stability of the stationary vortex solitons described by the system (5) is an important issue. In general, the stability analysis of vortices in nonlinear models is a complicated and, generally speaking, unsolved problem. Instability can develop due to the presence of unstable eigenmodes localized near the vortex core and, in the one-dimensional case, this type of instability of *dark solitons* leads to the soliton motion, i.e., it is a *drift instability* (see, e.g., Ref. [5] and references therein). Since moving vortices with nonzero minimum intensity (similar to grey solitons) do not exist, similar drift instability is not observed for vortices. The main instability that is usually associated with a vortex soliton originates from the instability of the nonlocalized background field.

The analysis of modulational instability of the background field can be carried out in a general form. First, we write Eqs. (2) and (9) in the form

$$i \frac{du}{dz} + s \nabla^2 u + \frac{\partial \mathcal{F}}{\partial u^*} = 0, \quad (15)$$

$$i \sigma \frac{dw}{dz} + s \nabla^2 w + \frac{\partial \mathcal{F}}{\partial w^*} = 0,$$

with \mathcal{F} defined as

$$\begin{aligned} \mathcal{F} \rightarrow \mathcal{F}_1 = & -|u|^2 + \frac{1}{2}(u^2 w^* + u^{*2} w) - \alpha |w|^2 \\ & + \chi \left(\frac{1}{8} |u|^4 + 2|w|^4 + \rho |w|^2 |u|^2 \right), \end{aligned} \quad (16)$$

for the model of competing nonlinearities, or

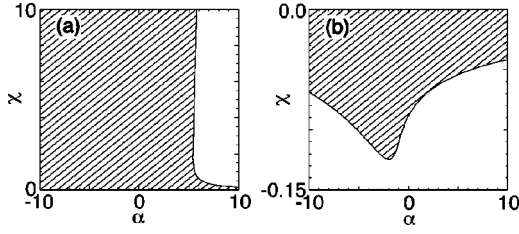


FIG. 1. Existence domains for the modulationally stable background modes of the system (2) for (a) $s = -1$ and $\chi > 0$; (b) $s = +1$ and $\chi < 0$.

$$\mathcal{F} \rightarrow \mathcal{F}_2 = -|u|^2 + \frac{s}{9}(u^3 w^* + u^{*3} w) - \alpha |w|^2 + s \left(\frac{1}{18}|u|^4 + \frac{9}{2}|w|^4 + 2|w|^2|u|^2 \right), \quad (17)$$

for the model of the third-harmonic generation. We look for stability of the background wave solution (U_0, W_0) defined by Eq. (11), and linearize Eq. (15) around this stationary solution substituting

$$\begin{aligned} u &= U_0 + a e^{i\mathbf{k}\cdot\mathbf{r} + i\omega z} + b e^{-i\mathbf{k}\cdot\mathbf{r} - i\omega z}, \\ w &= W_0 + c e^{i\mathbf{k}\cdot\mathbf{r} + i\omega z} + d e^{-i\mathbf{k}\cdot\mathbf{r} - i\omega z}. \end{aligned} \quad (18)$$

As a result, we obtain a system of linear equations for a, b^*, c , and d^* leading to the characteristic equation

$$\begin{vmatrix} A_{u^*,u} - \Omega & A_{u^*,u^*} & A_{u^*,w} & A_{u^*,w^*} \\ A_{u,u} & A_{u,u^*} + \Omega & A_{u,w} & A_{u,w^*} \\ A_{w^*,u} & A_{w^*,u^*} & A_{w^*,w} - \Omega & A_{w^*,w^*} \\ A_{w,u} & A_{w,u^*} & A_{w,w} & A_{w,w^*} + \Omega \end{vmatrix} = 0.$$

Here the nondiagonal elements are given by $A_{n,m} \equiv (\partial^2 F / \partial n \partial m)|_{u=U_0, w=W_0}$ where $n, m = u, u^*, w, w^*$, and in the diagonal matrix elements $A_{n,n^*} \equiv (\partial^2 F / \partial n \partial n^*)|_{u=U_0, w=W_0 - |\mathbf{k}|^2}$. Solving the characteristic equation with respect to Ω , we conclude the modulational instability analysis: purely real Ω solutions for all positive $|\mathbf{k}|^2$ (with other parameters fixed) indicate a modulationally stable background for this fixed set of the parameters. Below, we present the results of the modulational instability analysis for two cases of the parametric two-wave interaction.

IV. COMPETING NONLINEARITIES

Analysis of modulational instability for the system (2) has been briefly presented in Ref. [11]. Below we repeat the main steps of that analysis for the completeness of this paper. Solutions of Eq. (2) for background waves can be found by solving the coupled algebraic equations:

$$\begin{aligned} 12\chi W_0^3 + 12W_0^2 + W_0(\alpha - 8 + 2\chi^{-1}) &= 2\chi^{-1}, \\ U_0^2 &= 4(1 - W_0)\chi^{-1} - 8W_0^2, \end{aligned}$$

for real U_0 and W_0 . There exist up to *three such solutions* with both amplitudes U_0 and W_0 being nonzero. Performing

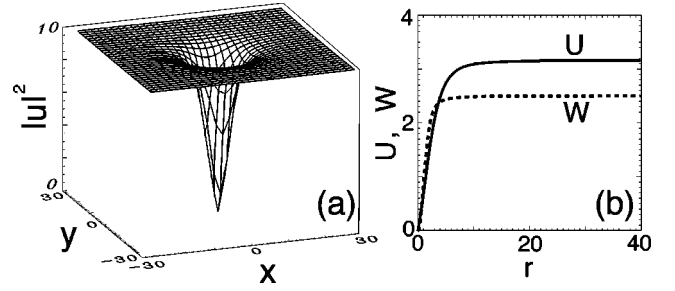


FIG. 2. An example of a two-component vortex soliton supported by competing nonlinearity ($\alpha = -2.5$, $\chi = -0.1$, and $s = +1$). In (a) only the vortex of the fundamental harmonic field is shown.

the analysis of modulational instability for each of the three solutions at $s = \pm 1$, we find that there exists only *one modulationally stable mode*. The parameter domains where such a solution exists are presented in Figs. 1(a) and 1(b). Note, that $\text{sign}(s\chi) = \text{sign}\chi^{(3)}$ and thus modulationally stable solutions exist only for $\chi^{(3)} < 0$. Importantly, the amplitude of the modulationally stable background diverge in the limit $\chi \rightarrow 0$ so that the stable background solution exists exclusively due to *mutual action of quadratic and cubic nonlinearities*. Other nonlinear modes are modulationally unstable in the whole domain of their existence and they are not presented in Figs. 1(a) and 1(b). Modulational stability in the limit of large negative $\chi^{(3)}$ [e.g., for $s = -1$ and $\chi > 0$, see Fig. 1(a)], is not surprising because stable dark solitons are known to exist in a defocusing Kerr medium without quadratic nonlinearity. Here, we are interested in the case when the effective nonlinearity is predominantly quadratic, i.e., $|\chi U_0| \sim |\chi W_0| \ll 1$. We found that this condition can only be satisfied for $s = +1$ where modulationally stable background waves of moderate amplitudes exist for relatively small values of negative χ [see Fig. 1(b)].

Using the numerical relaxation technique, we have found that a continuous family of two-component vortex solitons exists in the whole region of the existence of modulationally stable background waves shown in Figs. 1(a, b). Figures 2(a) and 2(b) present an example of such a vortex soliton.

Analysis of the vortex asymptotics demonstrates that halo-vortices can exist in Eq. (2) only if $s = -1$ and $\chi > 0$, in the narrow domain shown in Fig. 3. Both terms with B and B_2 factors in the asymptotic expansion (12) contribute to the formation of the halo (i.e., both BW_0 and B_2W_0 products are negative).

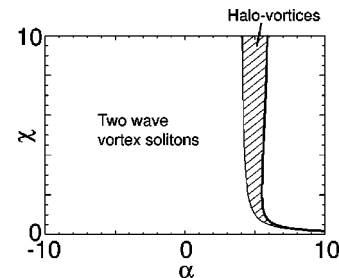


FIG. 3. Region of the existence of halo-vortices in the model of competing nonlinearities, $s = -1$.

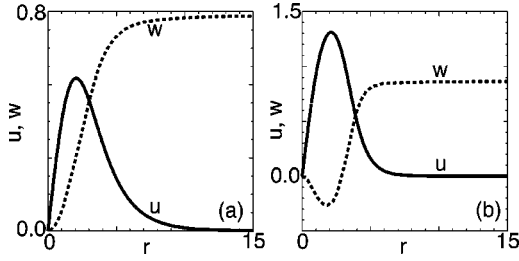


FIG. 4. Examples of a ring-vortex soliton ($s = -1$, $\chi = 1$) for (a) $\alpha = 1.4$ and (b) $\alpha = 3$. Solid, FH wave; dashed, SH wave.

Ring-vortex solitons can also exist in the model (2), see Figs. 4(a) and 4(b) and Figs. 5(a) and 5(b). Variational analysis allows us to find an approximate expression for the bifurcation curve where such solutions appear, $(2 - \alpha) = \sqrt{\alpha/\chi}$. As α increases, the maximum of the bright-ring amplitude approaches the value U_0 of two-wave modulationally stable parametric plane waves. At the values of r where U approaches U_0 , the second component, W , also approaches U_0 [see Fig. 4(b)].

Such ring-vortex solitons can be unstable due to modulational instability of the background wave $U_0 = 0, W_0^2 = \alpha/4\chi$. For example, for $s = -1, \alpha > 0$, modulational stability is defined by the condition $(\alpha - 2) > \sqrt{\alpha/\chi}$. The regions of the existence of modulationally stable one-component plane waves and ring-vortex solitons of Eq. (2) are presented in Fig. 6.

Existence of two-component stable vortex solitons composed of parametrically coupled fields suggests that such vortices can be excited in the process of the harmonic generation. In Fig. 7, we present the numerical simulation results supporting this idea. We launch a mode of the fundamental frequency without a seeded second harmonic assuming the condition of phase-matching. The vortex soliton dynamics is simulated using a split-step beam propagation method (BPM). To solve the problem of the vortex phase geometry, we simulate a system of four vortices, arranged such that horizontally and vertically adjacent vortices are opposite in charge. Lines of equal phase are chosen to correspond to the lines of the force of an equivalent system of electrostatic point charges. With the periodic boundary conditions imposed by BPM, this configuration means that, in fact, an infinite array of vortices is simulated. Figure 7 shows the vortex generation by an input fundamental mode with single-

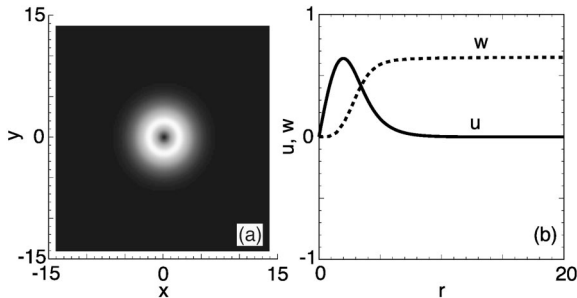


FIG. 5. (a) Intensity profile of the first harmonic, and (b) the amplitude profile of a ring-vortex soliton ($\alpha = 1.7$, $\chi = 1$, and $s = -1$) for the fundamental (solid) and second-harmonic (dashed) modes.

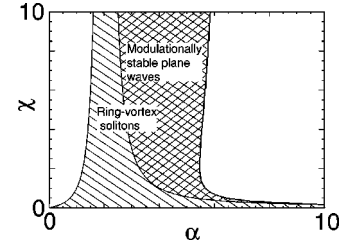


FIG. 6. Region of existence for ring-vortex solitons at $s = -1$ and $\chi > 0$. Left curve, $(2 - \alpha) = \sqrt{\alpha/\chi}$, is defined by a bifurcation where a bright component appears. Middle curve is a critical threshold that divides modulationally stable and unstable solutions. Right-hand side curve is the boundary for the existence of two-component parametric plane waves.

charged vortices. Due to phase matching with the second harmonic, we observe a generation of double-charge vortices in the harmonic field (see the plots at $z = 1$) and then periodic oscillations of the two-component background and the vortex profiles near a stationary state corresponding to a lattice of two-component vortex solitons (see the plots at $z = 10$ as an example of such dynamics).

V. THIRD-HARMONIC GENERATION

Vortex solitons of Eq. (9) have fewer parameters in comparison with the parametric vortices described by Eq. (2), and thus they can be analyzed much more easily numerically. These vortex solitons are found in the whole region of the existence of modulationally stable plane waves, i.e., for $\alpha < \alpha_{th} \approx 14.509$. Examples of such vortex solitons are shown in Figs. 8(a) and 8(b).

A third-harmonic component of the vortex solitons has a nonmonotonic tail for $10.85 < \alpha < 14.509$, however it can only be called a halo vortex for the interval $11.26 < \alpha < 14.509$, where the absolute value of a local extremum in the structure of the vortex tail is greater than the corresponding plane wave background value W_0 . The halo is becoming more pronounced as $\alpha \rightarrow 14.509$. An example of a halo-vortex soliton of Eq. (9) is shown in Fig. 9.

Ring-vortex solitons have also been found for the model (9), see Fig. 10. In this case, a variational analysis allows us to find an approximate analytical result for the bifurcation

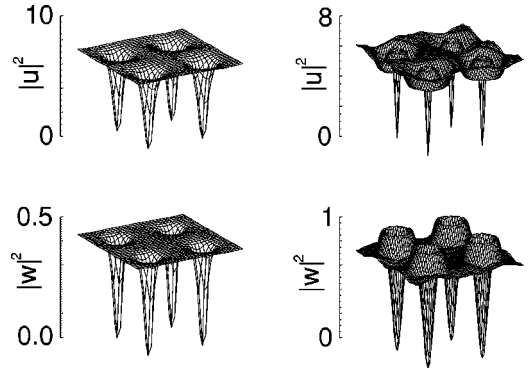


FIG. 7. Generation of two-component parametric vortex solitons by the fundamental vortices. Profiles of the fundamental (upper row) and second-harmonic (lower row) fields are shown at $z = 1$ (left column) and $z = 10$ (right column).

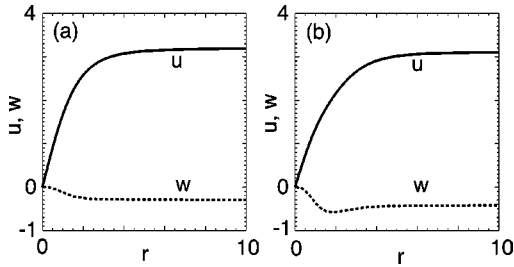


FIG. 8. Examples of two-component vortex solitons supported by the third-harmonic generation at $s = -1$: (a) $\alpha = 9$, and (b) $\alpha = 13$.

point ($s = -1$) where a ring-like mode is guided by the vortex

$$\alpha_{\text{bif}} = \frac{(\gamma/\rho)}{\left\{ 1 - \frac{2}{9} \left[1 - \frac{\gamma}{2\rho N^2 m^2} (1 + 2m^2) \right]^3 \right\}}.$$

For $\gamma = 9, \rho = 2, N = 3$, and $m = 1$ this gives $\alpha_{\text{bif}} \approx 4.52$, which agrees well with numerical data. We also find that, in general, coupled ring-vortex solitons exist for $\alpha > 4.5$, and for each such value of α (except $\alpha = \alpha_{\text{bif}}$) there exist *two different types of ring-vortex solitons* (see Fig. 10). As the parameter α decreases, the maximum of the bright ring in the fundamental mode approaches the value of U_0 of the two-wave modulationally stable background field. Again, as it has been observed for the model of competing nonlinearities, at values of r where U approaches U_0 , the vortex component W deforms significantly approaching the corresponding plane-wave amplitude W_0 . We note that *all these ring-vortex solitons are modulationally stable*, because, in the framework of Eq. (9), modulational instability does not occur for one-component plane wave solutions.

VI. CONCLUDING REMARKS

We have analyzed two-component vortex solitons supported by parametric wave mixing in a nonlinear optical medium. We have considered two classes of such vortex solitons. In the first case, we have studied the existence, structure, and stability of vortex solitons supported by phase-matched interaction between the fundamental and second-harmonic waves in a quadratic medium, and the effect of the next-order cubic nonlinearity has been taken into account for suppressing modulational instability of the supporting plane-

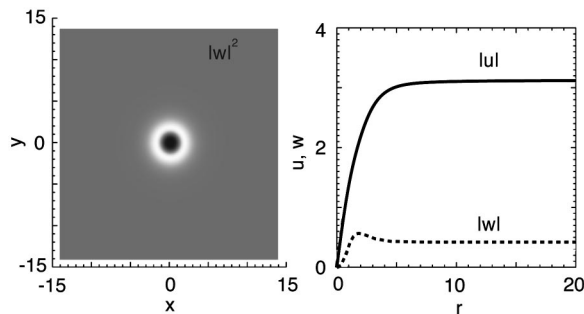


FIG. 9. Example of a halo-vortex soliton as a stationary solution of Eq. (9) for $s = -1$ and $\alpha = 13$.

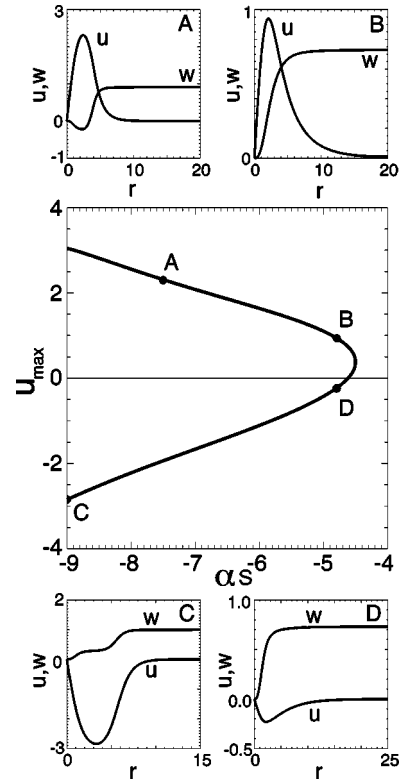


FIG. 10. A family of ring-vortex solitons shown in the middle plot as the maximum of the bright-ring amplitude u_{max} vs αs . Filled circles A, B and C, D correspond to the vortex profiles shown above and below, respectively.

wave background. In the second case, we have considered how the vortex parameters, structure, and stability are modified due to the process of third-harmonic generation when the phase-matched wave interaction generates a corresponding multicharge vortex component in a harmonic field. In particular, we have predicted the so-called ‘‘halo-vortex’’ consisting of a two-wave vortex core surrounded by a bright ring on a nonvanishing background. Additionally, we have analyzed the waveguiding properties of a vortex soliton in the case when it guides a harmonic field due to a phase-matched parametric interaction. A rigorous analysis of the stability of these parametric vortex solitons is still an open problem, as well as the effect of walk-off on the vortex existence and stability.

As for experimental verifications of the vortex solitons described above, we would like to mention that, at least in the low-intensity regime, parametric vortices have already been observed in nonlinear optics. A possibility of SHG by a beam with a vortex was first mentioned and experimentally verified in Ref. [6], where a vortex of the topological charge $m = 2$ was found in the second-harmonic wave when the fundamental wave contained a vortex of the topological charge $m = 1$. The similar results on SHG have been presented by Dholakia *et al.* in Ref. [7], whereas more complicated processes of sum-frequency mixing with beams carrying phase singularities were reported by Beržanskis *et al.* [8,9]. It is worth noticing that in all of those observations the different harmonics experienced noticeable walk-off that makes the stationary structures difficult to observe, also introducing novel features in the vortex dynamics. In particular, for a

collinear type I phase-matched SHG with an input beam carrying a single-charge vortex, Matijošius *et al.* [19] observed two intensity zeroes in the second-harmonic field with the separation of two SHG vortices due to walk-off. Thus, we can expect that stationary two-component vortex solitons discussed above can be observed in typical upconversion experiments when a high-intensity beam undergoes frequency doubling simultaneously with the creation of a phase singularity produced by a phase mask at the input, similar to the experiments mentioned above which were performed at moderate powers. *Stability* of those vortex solitons requires small (or zero) walk-off and a small defocusing Kerr nonlinearity of an optical material at both (or at least fundamental wave) frequencies.

Additionally, we would like to mention that the parametrically coupled equations of competing nonlinearities, similar to Eq. (2) analyzed above, have been recently introduced by Heinzen *et al.* [20] to describe the dynamics of *coupled atomic and molecular Bose-Einstein condensates*, leading to a kind of “superchemistry” in which the formation of molecules is a controlled parametric quantum process. In spite of the fact that both atomic and molecular condensates should be considered in a trapping external potential [21], many of the features of the coupled stationary states, including all the types of the vortex states introduced above, are expected to exist in the model of atom-molecular

condensates as well, providing a much broader view of the phenomenology of parametric vortex solitons.

At last, we expect that the concept of the two-component parametric vortices, generated and supported by the third-harmonic generation process, can be important in the so-called *third-harmonic microscopy* (see, e.g., Ref. [22]) where an image is rendered using a series of cross-sectional images produced by third-harmonic generation within the specimen. Vortices can then be formed due to the development of caustics [2] in the reflected harmonic field, indicating the regions of highly concentrated inhomogeneities. This technique is based on the fact that the nonlinear susceptibility of solid media vary over many orders of magnitude, compared with linear refractive index changes that vary in a relatively small range.

ACKNOWLEDGMENTS

The authors thank O. Bang, P. DiTrapani, B. Ivanov, L. Pismen, A. Piskarskas, Y. Silberberg, V. Smilgevičius, and I. Towers for useful discussions of the properties of multicomponent and parametric vortices and harmonic generation. The work has been supported by the Australian Photonics Cooperative Research Center and the Australian Research Council. A brief summary of the results has been presented at the OSA Annual Meeting in Baltimore.

-
- [1] J.F. Nye and M.V. Berry, Proc. R. Soc. London, Ser. A **336**, 165 (1974).
- [2] J. F. Nye, *Natural Focusing and Fine Structure of light: Caustics and Wave Dislocations* (Institute of Physics Publishing, Bristol, 1999).
- [3] V.L. Ginzburg and L.P. Pitaevsky, Zh. Éksp. Teor. Fiz. **34**, 1240 (1958) [Sov. Phys. JETP **7**, 858 (1958)]; see also L.P. Pitaevsky, *ibid.* **40**, 646 (1961) [**13**, 451 (1958)].
- [4] L.M. Pismen, *Vortices in Nonlinear Fields* (Oxford University Press, Oxford, 1999).
- [5] See, e.g., Yu.S. Kivshar and B. Luther-Davies, Phys. Rep. **298**, 81 (1998).
- [6] I.V. Basistiy, V. Yu. , Bazhenov, M.S. Soskin, and M.V. Vashnetsov, Opt. Commun. **103**, 422 (1993).
- [7] K. Dholakia, N.B. Simpson, M.J. Padgett, and L. Allen, Phys. Rev. A **54**, R3742 (1996).
- [8] A. Beržanskis, A. Matijošius, A. Piskarskas, V. Smilgevičius, and A. Stabinis, Opt. Commun. **140**, 273 (1997).
- [9] A. Beržanskis, A. Matijošius, A. Piskarskas, V. Smilgevičius, and A. Stabinis, Opt. Commun. **150**, 372 (1998).
- [10] A.V. Buryak and Yu.S. Kivshar, Phys. Rev. A **51**, R41 (1995); Opt. Lett. **20**, 834 (1995); S. Trillo and P. Ferro, *ibid.* **20**, 438 (1995).
- [11] T.J. Alexander, A.V. Buryak, and Yu.S. Kivshar, Opt. Lett. **23**, 670 (1998).
- [12] A.V. Buryak, Yu.S. Kivshar, and S. Trillo, Opt. Lett. **20**, 1961 (1995).
- [13] O. Bang, Yu.S. Kivshar, A. V. Buryak, A. De Rossi, and S. Trillo, Phys. Rev. E **58**, 5057 (1998).
- [14] R.A. Sammut, A.V. Buryak, and Yu.S. Kivshar, J. Opt. Soc. Am. B **15**, 1488 (1998).
- [15] See, e.g., M. Haelterman and A.P. Sheppard, Chaos Solitons Fractals **4**, 1731 (1994); A.P. Sheppard and M. Haelterman, Opt. Lett. **19**, 859 (1994).
- [16] M. Segev and G. Stegeman, Phys. Today **8**, 42 (1998).
- [17] A.G. Truscott, M.E.J. Friese, N.R. Heckenberg, and H. Rubinsztein-Dunlop, Phys. Rev. Lett. **82**, 1438 (1999).
- [18] A. W. Snyder and J. D. Love, *Optical Waveguide Theory* (Chapman and Hall, London, 1983).
- [19] A. Matijošius, A. Piskarskas, V. Smilgevičius, and A. Stabinis, CLEO '99, OSA Technical Digest (OSA, Washington, D.C., 1999), p. 304.
- [20] D.J. Heinzen *et al.*, QELS '99, OSA Technical Digest (OSA, Washington D.C., 1999), p. 54.
- [21] See, e.g., F. Dalfovo, S. Giorgini, L.P. Pitaevskii, and S. Stringari, Rev. Mod. Phys. **71**, 463 (1999).
- [22] Y. Barad, H. Eisenberg, M. Horowitz, and Y. Silberberg, Appl. Phys. Lett. **70**, 922 (1997).